



移动扫码阅读

陈 健,李 洋,刘文中,等.岩浆侵入对煤结构的影响评述[J].煤炭科学技术,2021,49(6):170-178.doi:10.13199/j.cnki.cst.2021.06.020

CHEN Jian, LI Yang, LIU Wenzhong, et al. Review on impacts of igneous intrusion in coal measures on coal texture [J]. Coal Science and Technology, 2021, 49(6): 170-178. doi: 10.13199/j.cnki.cst.2021.06.020

岩浆侵入对煤结构的影响评述

陈 健,李 洋,刘文中,江佩君,曾 建,陈 萍

(安徽理工大学 地球与环境学院,安徽 淮南 232001)

摘要:岩浆侵入煤系地层导致煤发生接触变质作用,形成天然焦,降低煤经济价值,增加自然和瓦斯突出风险,改变煤层气赋存条件,还被认为是地史时期全球气候变化和生物绝灭的重要触发因素。为揭示岩浆侵入过程煤结构的变化规律,文章从煤层宏观结构构造到微观显微组分,从原始沉积结构的变化到新形成的特征结构,全面系统论述了岩浆侵入对煤结构的影响。岩浆高温、侵位压力、热液流体等因素导致煤层结构构造和煤显微组分发生显著改变,发育微孔裂隙、脱挥发孔或囊状结构、各向同性焦、各向异性焦、热解碳、石墨球粒和焦化沥青质等。受岩浆侵入影响煤层煤结构的变化规律是确定接触变质晕范围和气体赋存条件的科学基础,在热变质煤资源的安全开采和综合利用方面亦具重要现实意义。

关键词:岩浆侵入;煤结构;煤岩组成;热变煤

中图分类号:P618.11 **文献标志码:**A **文章编号:**0253-2336(2021)06-0170-09

Review on impacts of igneous intrusion in coal measures on coal texture

CHEN Jian, LI Yang, LIU Wenzhong, JIANG Peijun, ZENG Jian, CHEN Ping

(School of Earth and Environment, Anhui University of Science and Technology, Huainan 232001, China)

Abstract:The igneous intrusion in coal measures resulted in a contact metamorphism of coal to form a natural coke or a thermally altered coal. Coal metamorphism by igneous intrusion reduces the value of coal, increases the risk of spontaneous combustion and gas outburst, worsens the trapping condition of coalbed methane, and is also considered as one cause for the global climate change and mass extinction in certain geological history. To reveal the evolution of coal texture during igneous intrusions, the impacts of igneous intrusion in coal measures on coal texture were systematically elucidated from a macroscopic coalbed texture to the microscopic coal macerals and from the original sedimentary textures to the metamorphic features in this paper. Due to the high temperature, increased static pressure, and hydrothermal fluids during igneous intrusion, the texture and structure of coalbed and coal macerals were thermally altered. Moreover, the neo-formed textures, including fractures, devolatilization cavities and vacuoles, isotropy, anisotropy, pyrolytic carbons, graphitic spherulites, and coked bitumen, were developed. The evolution of coal texture caused by an igneous intrusion provides the scientific information about the aureole of contact metamorphism and the occurrence conditions of coalbed methane, and is of practical significance for the safe and comprehensive utilization of thermally altered coals.

Key words:igneous intrusion; texture of coal; coal petrology; thermally altered coal

0 引言

岩浆侵入煤层导致煤变质成天然焦,经济价值降低^[1-2],孔裂隙发育,增加煤自燃和瓦斯突出风险^[2-4],改变煤层气赋存条件^[4-7],接触变质过程释放的热成CH₄和CO等还被认为是地史时期全球气

候变化和生物绝灭的重要因素^[8-12]。岩浆侵入对煤物质组成的影响是煤地质学领域研究的热点问题,国内外学者尤为关注,成果较丰富,岩浆侵入可改变煤的光学、物理和化学性质:煤级提升,镜质组反射率增加^[13-14],镜质组形成中间相^[15]、各向同性和各向异性焦^[16-17]、类脂组消失^[18]、热解碳沉积^[16]等,

收稿日期:2021-03-15;责任编辑:郭 鑫

基金项目:国家自然科学基金面上资助项目(41972173);安徽省杰出青年科学基金资助项目(1908085J14)

作者简介:陈 健(1984—),男,四川仪陇人,副教授,博士生导师,博士。E-mail:cscchenjian@163.com

碳球粒形成^[15]、发育流动和气孔构造^[16]。狭义的煤结构是指煤岩成分的形态、大小、厚度、植物组织残迹,以及它们之间相互关系所表现出来的特征^[19],广义的煤结构还应该包括煤层结构。在全面收集国内外相关文献资料的基础上,结合作者的研究经验,系统论述了岩浆侵入对煤结构构造和煤显微组分的影响,深入讨论了煤变质结构的形成原因和影响因素,以期为煤地地质学领域的基础理论研究和热变质煤资源的综合利用提供科学依据。

1 岩浆侵入对煤结构构造的影响

1.1 岩浆侵入对煤结构的影响

1.1.1 煤层结构的变化

煤的力学强度小于含煤地层其他岩石,因此,上涌岩浆易沿煤层侵入,岩浆侵位将改变煤层结构,煤层分叉、变薄甚至被完全吞蚀,从而破坏煤层的连续性和完整性,减少煤炭资源储量,影响煤矿安全,如山东济宁煤田金乡勘探区^[20-21]、黄河北煤田^[22]和河南豫东地区^[23]。

岩浆侵入对煤层结构的影响程度与岩浆的侵入模式有关。一般而言,由于岩床的岩浆量和与煤层的接触面积大,其顺层侵入对煤层结构的影响远大于其他模式;且在岩床沿煤层顶、底板侵入模式中,沿煤层底板侵入对煤层影响更大,而沿煤层顶板侵入的影响较小^[22];以岩脉等形式顺层、垂直或倾斜侵入煤层的影响范围较小^[20-21]。

1.1.2 孔裂隙的变化

岩浆侵入煤层的接触热变质作用,主要是挥发分逸散和温度剧变,导致煤层孔裂隙发育,淮南煤田潘三矿1煤层岩床侵入(反射光)如图1所示,孔裂隙一般随与侵入体距离的减少而增加。热变质煤微孔裂隙的发育,提供瓦斯赋存空间,增加瓦斯吸附

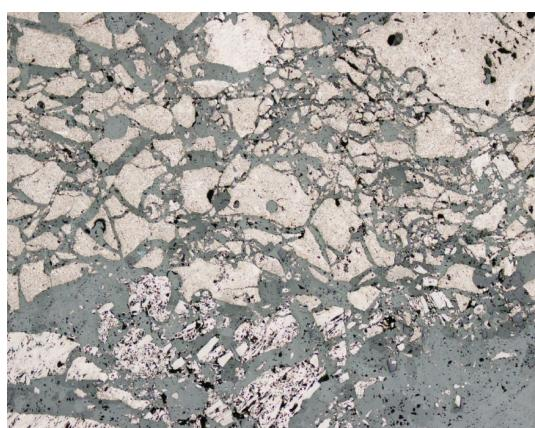


图1 热变质煤中的网状裂隙

Fig.1 Fracture network in thermally altered coals

量^[20-22],影响煤炭安全开采。

红阳、邯郸和淮北煤田受岩浆侵入影响的热变质煤越接近侵入体,变镜质组中脱挥发孔和干燥微裂隙便越发育,尤其是胶质结构镜质体、团块凝胶体、胶质碎屑体^[5];淮北煤田卧龙湖矿岩床侵入导致煤的微孔体积和表面积在不同热演化区差异变化,在热演化一区,微孔体积和表面积显著减小,而在热演化二区,微孔体积和表面积稍增加^[4],海孜矿巨厚岩床侵入导致热变质煤的比表面积和孔体积均增加,且孔的连通性增强^[24];辽宁大兴煤矿岩浆热变质煤的孔隙度、孔体积和孔径均较未变质煤大^[25];美国 Illinois 盆地岩浆侵入煤的接触变质分4个阶段,其中,第2阶段热变质煤孔隙不均匀发育,呈浮岩状,孔径和孔形态变化,在接触带由于挥发分剧烈变化和温度最快速上升,孔径最大^[26],接触变质作用对 Springfield 煤层孔隙有较大影响,尤其是微孔,近侵入体,微孔体积先增后减^[27];印尼 South Sumatra 盆地安山岩岩床侵入煤层导致 BET 表面积下降,而微孔表面积增加^[28]。

美国科罗拉多州 Purgatoire 河谷煌斑岩岩床侵入导致热变质煤裂隙强烈发育^[29],而煌斑岩中的煤捕虏体因结焦过程体积减小,裂隙发育^[30];澳大利亚 Gunnedah 盆地辉绿岩侵入导致 Black Jack 群煤层微裂隙发育^[31];印度 Jharia 煤田 Ena 矿 XIII 煤层和 Alkusa 矿 XIV 煤层上部微孔裂隙极度发育与挥发分快速释放导致煤级的急剧提升有关^[1];莫桑比克 Chipanga 煤层上部由于侵入体的热效应和侵位压力,发育裂隙网,而煤层下部不发育^[32]。

1.1.3 囊状结构(脱挥发孔)的形成

岩浆接触热变质作用导致煤有机质活性成分裂解,挥发分逸散,形成囊状结构(脱挥发孔)(图2)。河北峰峰-邯郸煤田C4煤层由于岩浆热液作用,显微组分囊状结构发育良好,且为后生方解石充填^[33];江西乐平沿沟矿二叠系热变质煤大量发育囊状结构,且被碳酸盐矿物和方沸石充填^[34];安徽淮北杨柳矿岩床侵入煤层,形成大量脱挥发孔^[35];印度二叠系煤层云母橄榄岩侵入导致囊状结构发育,为后生方解石和石英充填^[26],Jharia 煤田热变质煤挥发分逸散的重要证据为不同大小孔或洞状囊泡的发育^[1],East Bokaro 煤田热变质煤镜质组存在脱挥发囊泡^[36];澳大利亚昆士兰州东部 Collinsville 煤系岩浆侵入热变质煤囊泡高度发育,尤其是煤与侵入体的接触带^[37],Gunnedah 盆地辉绿岩侵入导致煤层存在大量脱挥发孔^[31];美国 Illinois 盆地 Springfield 煤层在离接触带 2 m 处镜质组中便可见

热成脱挥发孔^[13],且靠近岩脉,脱挥发囊泡普遍增多^[14,17-18],Herrin 煤层热变质煤焦化镜质组亦发现脱挥发囊泡,且在热变质晕中随煤级提升而增多^[38-39],Danville 煤层脱挥发囊泡发育表明挥发分的释放^[40];科罗拉多州 Pitkin 郡 Dutch Creek 矿岩脉侵入导致在距接触带 40 cm 处即可见囊泡发育,在距接触带 30 cm 处囊泡由于热变质煤的流动性而拉长,在距接触带 17 cm 处煤样中囊泡大量存在,为后生方解石充填^[41]。

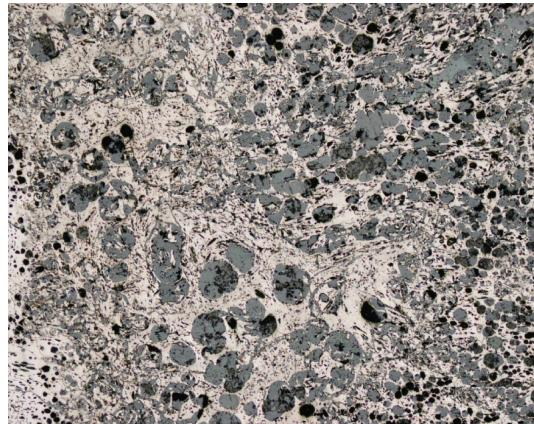


图 2 热变质煤中的脱挥发孔

Fig.2 Devolatilization vacuoles in thermally altered coal

印度天然焦有大量孔隙,并发育不同形状和大小的囊泡,其大小与形态和煤级、侵入时长和规模、与侵入体的距离、加热与冷却程度、挥发分逸散条件等因素有关^[42];印尼 Suban 煤层所有煤样均发育孔隙和囊泡,表明岩浆侵入热变质的快速脱挥发过程^[43];南非 Highveld 煤田 4L 煤层近岩脉的热变质煤中镜质组由于挥发分逸散,囊状结构发育^[44];美国 Purgatoire 热变质煤区均有囊泡存在,且其数量和大小沿侵入体方向增加,全区囊泡发育表明岩浆侵入后煤的流变程度足以囊泡化,且囊泡内部气压大于围岩压力^[29],该区煌斑岩煤捕虏体中囊泡数量众多,越接近岩床数量越多^[30],Raton 组煤基天然焦脱挥发囊泡发育^[15];匈牙利 Mecsek 热变质煤中存在微小的圆形或椭圆形小孔(<10 μm),其形成与挥发分释放有关^[45]。

1.2 岩浆侵入对煤构造的影响

煤层岩浆侵位伴随局部温度和压力的增加,改变煤的力学性能,煤原始沉积构造变化,发生韧性变形,形成各类褶皱;或发生塑性变形,形成不同规模流动构造;或由于冷却体积变化和扩张空间受限等因素,发育柱状节理。

1.2.1 褶皱的形成

莫桑比克 Moatize 盆地二叠系煤层上部热变质

煤的层理强烈褶皱,其中,以镜质组为主的亮煤带褶皱发育,而暗煤带变形并形成裂隙^[32]。一般而言,褶皱变形先于裂隙发育,由于侵入岩浆的高温和增加的压力,煤先发生韧性变形,随后冷却并产生裂隙^[32]。美国 Illinois 盆地上石炭统 Springfield 含煤段岩脉侵入形成的热变质煤由于岩脉边界局部应力集中导致显微组分和煤岩带扭曲和重排^[13],科罗拉多州 Purgatoire 河谷热变质煤的主要结构特征为层理消失或扭曲变形^[29];澳大利亚 Sydney 盆地带状热变质煤区,原始煤岩层理一定程度褶皱,仍模糊可见,随与侵入体距离的减小,层理变形并破裂,煤变质过程释放的挥发分无逸散和缺乏可扩张空间是层理变形的主要原因^[46]。

1.2.2 流动构造的形成

由于岩浆高温,接触的煤发生塑性变形,形成各种流动构造^[42](图 3),此外,不同形状和大小的拉长流动构造还表明岩浆侵入伴随较高压力的影响^[16],如印度 Jharia 煤田,由于较高压力,热变质煤中流动构造发育^[1],XIV 煤层的定向流动构造表明其在高温高压条件下的原位碳化过程^[16]。



图 3 热变质煤中发育的流动构造

Fig.3 Flow structures in thermally altered coal

1.2.3 柱状节理的发育

岩浆侵入煤层后,岩浆和煤冷却,煤在快速冷却结焦过程中,体积减小,发育六边形柱状节理。辽宁阜新盆地下白垩统辉绿岩侵入形成的热变质煤六边形柱状节理发育^[47];印度 Jharia 和 Raniganj 煤田的热变质煤带状构造完全破坏,在垂直于接触面的方向显著发育柱状节理^[48-49];美国科罗拉多州 Purgatoire 河谷 Raton 组岩床中煤捕虏体明显可见六边形柱状节理^[15],阿拉斯加中南部 Matanuska 煤田古新统 Chickaloon 组热变质煤柱状节理发育,且节理面与侵入体表面垂直^[50];南非辉绿岩侵入形成的热变质煤柱状节理亦普遍发育^[51]。

2 岩浆侵入对煤显微组分的影响

煤碳化过程中,显微组分分成2组,第1组变成液态,发育各向异性,形成颗粒镶嵌结构,如类脂组和烟煤的镜质组(胶质碎屑体和胶质结构镜质体);第2组几乎保持非液态,发育各向同性或基本不发育各向异性,如惰质组和低煤级煤的镜质组^[52]。一般而言,在岩浆侵入煤层的接触热变质过程中,镜质组转变成各向同性或各向异性焦,类脂组消失,而惰质组基本不变^[14,18]。印度 Jharia 煤田弱热变质煤(前塑性阶段,温度<300 °C)中,镜质组较未变质的反射率更高,类脂组开始消失,惰质组基本未受影响;在中等变质煤(塑性阶段,300~500 °C)中,反应性组分,包括镜质组和类脂组,形成中间相和熔化天然焦,类脂组消失,惰质组在结构上几乎无变化,仅反射率稍增加;在严重热变质煤(后塑性阶段,温度>500 °C)中,中间相、镶嵌结构、石墨球粒和热解碳形成,而惰质组的形态结构变化(变形或破裂),反射率稍增大^[1]。

2.1 镜质组的变化

山西大同煤田岩浆侵入导致镜质组转化为天然焦基质^[53];红阳、邯郸和淮北煤田煤在接触变质过程中,镜质组呈塑性,导致热变质煤有相当程度变形,且在朱庄矿、孟庄矿和红菱矿其含量随与侵入体距离的减小而减少^[5];英格兰北部 Yard 煤层接近岩脉,镜质组转变成各向同性焦^[54];美国 Illinois 盆地近岩脉煤和富有机质页岩中镜质组产生脱挥发孔,且随温度增加而发育各向同性和各向异性结构^[40];莫桑比克 Moatize 盆地 Chipanga 煤层镜质组变质,呈初始镶嵌结构^[32];印度 Ena 矿 XIII 煤层上部镜质组减少,相应各向异性组分和热解碳增多^[42];澳大利亚 Hunter Valley 二叠系煤岩脉侵入导致其镜质组完全转变成多孔各向异性镶嵌结构焦^[55]。

2.2 类脂组的变化

印尼 South Sumatra 盆地 Suban 热变质煤最明显的变化是类脂组含量降低^[43];印度二叠系煤层橄榄岩侵入导致孢子体、角质体和树脂体消失^[48];美国 Illinois 盆地 Danville 煤层在近橄榄岩岩脉的接触带类脂组消失,表明温度高于 300 °C^[40], Springfield 煤层近岩脉 3 m 处类脂组难辨别,荧光消失^[13,18],具体为当变质晕中煤 $R_{o,max} > 1.3\%$ 时,类脂组消失^[17,40,56],Herrin 煤层类脂组消失时的反射率为 1.36%^[38-39];在南非 Karoo 盆地 Highveld 煤田亦有相同发现,当变质晕中煤 $R_o > 1.35\%$ 时,类脂组消失^[44];山西大同煤田岩浆侵入导致类脂组消失或难

以识别^[53];然而,加拿大 British Columbia 省 Telkwa 煤变质残渣中部分类脂组仍保留原始形态^[52]。

2.3 惰质组的变化

红阳、邯郸和淮北煤田热变质煤中惰质组含量随与侵入体距离的减小而增加^[5];莫桑比克 Chipanga 煤层丝质体和半丝质体层变形,形成褶皱构造^[32];美国科罗拉多州 Purgatoire 河谷 Raton 组煤层上部真菌体普遍存在,为最抗热变质的显微组分^[29],所有变质煤样品中均有丝质体、微粒体和真菌体,且变化较小或无变化^[30], Pitkin 郡 Dutch Creek 矿离岩脉 6 cm 的热变质煤主要由惰质组组成^[41],然而,Springfield 煤层沿侵入体方向惰质组含量则降低,可能与原始煤的不均匀性或严重热变质煤中镜质组与惰质组难区分有关^[13],而 RAHMAN 等^[56]则发现无系统变化;南非 Highveld 煤田惰质组在热变质过程镜质组转化的情况下含量增加^[44];印尼 Suban 热变质煤惰质组的结构未改变^[43]。

2.4 各向同性和各向异性焦的形成

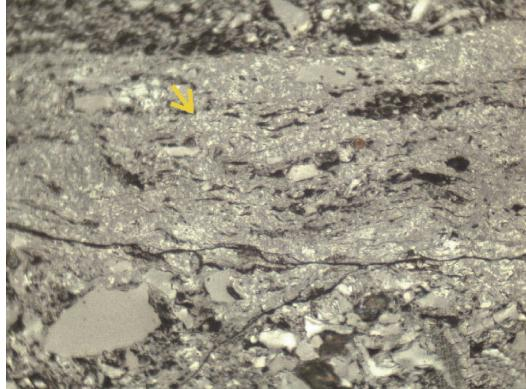
2.4.1 焦结构的类型

美国 Illinois 盆地 Springfield 煤层靠近岩脉,镜质组焦化作用增强,呈各向同性和各向异性焦^[14,56]。采用正交偏振器和抗折射物镜,各向同性焦呈红色或蓝色,而各向异性焦呈圆形镶嵌结构,具强双折射现象^[14]。

1)各向同性焦。根据粒径大小,各向同性焦分为细粒(<25 μm)、中粒(25~50 μm)和粗粒(>50 μm)^[16]。美国 Illinois 盆地 Danville 煤层橄榄岩岩脉侵入,形成各向同性焦^[40],Herrin 煤层在距侵入体约 1 m 处的变镜质组中见各向同性焦^[38,39];南非 Highveld 煤田 4L 煤层岩脉侵入形成各向同性焦^[44];澳大利亚 Collingsville 煤系离侵入体约 0.8 m 处镜质组具有各向同性^[37]。

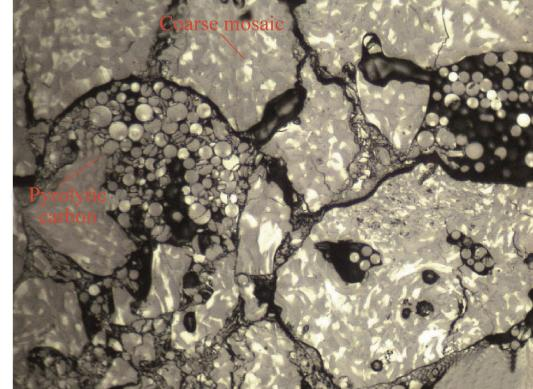
2)各向异性焦(镶嵌结构)。煤有机组分在热变质过程中形成不同大小具各向异性的均匀结构,称镶嵌结构(图 4),据粒径大小,分为细粒(<1.5 μm)、中粒(1.5~5 μm)和粗粒(5~10 μm)^[1,57]。美国 Springfield 煤层在离侵入体最近的样品中发育细粒镶嵌结构^[17,18,27,56,58-59],Raton 盆地热变质煤发育细粒至粗粒镶嵌结构^[60],Herrin 煤层距侵入体最近的样品(<0.4 m),发育初始和细粒圆形镶嵌结构^[39];印度 Jharia 煤田热变质煤发育细粒至粗粒镶嵌结构^[1,42],East Bokaro 煤田热变质煤镜质组见初始镶嵌结构^[36];澳大利亚 Collingsville 煤系煤与侵入体接触带细粒镶嵌结构发育^[37];莫桑比克 Chipanga 煤层镜质组带见初始镶嵌结构^[32];匈牙利 Mecsek

热变质煤中亦观察到由均质镜质体转化而成的镶嵌结构^[45];安徽淮北卧龙湖矿近岩床的煤具明显的热变质特征,即变镜质组的细粒镶嵌结构^[4],朔里矿岩床下热变质煤发育由细及粗的镶嵌结构^[61],石台矿热变质煤中见细-粗粒镶嵌结构^[62];河北峰峰-邯郸



(a) 细粒镶嵌结构

煤田热变质煤中亦见镶嵌结构^[33];江西乐平沿沟矿B4煤层热变质煤具初始镶嵌结构^[34];山西大同煤田严重热变质煤发育不同粒径的镶嵌结构,以细粒为主^[57];具异向光性的组分是岩浆热变质煤的“标志物”,甚至可作为井下预测岩浆岩的“标志”^[63]。



(b) 粗粒镶嵌结构及球状热解碳

图4 热变质煤的焦结构^[61]Fig.4 Coke textures in thermally altered coals^[61]

2.4.2 焦结构的成因

澳大利亚 Sydney 盆地热变质煤具密实的焦结构,发育小孔和厚腔壁,呈细粒、中粒镶嵌结构,与人工焦的结构不同,人工焦具有大孔和薄腔壁,呈极细粒各向同性镶嵌结构;粗粒镶嵌结构的形成与热变质过程充分预热和挥发分逸散受限有关^[46]。

2.4.3 焦结构发育的影响因素

1) 初始煤级。南极洲 Transantarctic 山热变质煤中各向同性焦表明岩浆侵入时煤级低于高挥发 A 烟煤($R_{max} < 0.7\%$),反射率在 0.7%~2.0% 时随煤级提升逐步形成圆形、透镜状、带状各向异性镶嵌结构,若反射率小于 0.5%,仅形成各向同性焦^[64];岩浆侵入时煤级为烟煤才能形成镶嵌结构,低煤级煤(褐煤)和高煤级煤(半无烟煤)均不能形成^[15]。

GOODARZI 等证实仅焦煤的碳化镜质组镶嵌结构明显发育,过低和过高煤级煤镜质组镶嵌结构较少;对具体有机组分而言,若升温速率相同,各向异性组分的变化取决于显微组分的成熟度^[46];南非 Highveld 煤田 4L 煤层的镜质组反射率约为 0.7%,岩脉侵入形成各向同性焦^[44];英格兰北部石英辉绿岩岩床侵入 Yard 煤层热影响区的烟煤($R_o = 1.5\%$)形成粒状镶嵌结构,当 $R_o > 1.5\%$ 时,未见镶嵌结构^[54];美国 Purgatoire 河谷 Raton 组未变质煤为高挥发烟煤,故其热变质煤发育中粒圆形镶嵌结构^[15],Springfield 煤层靠近岩脉,当镜质组反射率为 2.91% 时,见各向同性焦,而各向异性细粒镶嵌结构表明岩浆侵入时煤级为高挥发烟煤^[14],Herrin 煤层

初始和细粒圆形镶嵌结构发育的样品反射率大于 3.03%^[38]。

2) 煤岩组成。印度 Jharia 煤田 XIV 煤层热变质煤的各向异性组分源于反应性显微组分,如镜质组、类脂组、碎屑镜质体,而惰质组,包括半丝质体、丝质体、分泌体、粗粒体和微粒体,形成各向同性焦结构^[16]。

3) 温度。一般而言,初始镶嵌结构形成的温度应不低于 400 °C,完全形成镶嵌结构温度不高于 550 °C^[30]。美国 Purgatoire 河谷在煌斑岩岩床上部愈近岩床,镶嵌结构越发育,表明镶嵌结构形成与上升的温度有关,据氢含量计算该区初始镶嵌结构形成温度为 420~463 °C,细-粗粒镶嵌结构形成温度为 462~562 °C^[29~30];Illinois 盆地 Herrin 煤层热变质形成各向异性镶嵌结构,包括圆形、透镜状和带状,形成于 350~450 °C 的流态阶段^[38],Danville 煤层的细粒圆形镶嵌结构表明热变质温度接近 500 °C^[40],Springfield 煤层中细粒镶嵌结构形成温度高于 500 °C,而镜质组反射率数据估算变质温度约 370 °C^[13]。SINGH 等^[1]认为温度高于 500 °C,热变质煤将发育细粒至粗粒镶嵌结构^[1]。

4) 升温速率。岩浆侵入体规模越大,侵入时的背景温度越高,距侵入体一定距离的沉积物升温速率越小,从而导致粒状镶嵌结构的粒径越大,故粒状镶嵌结构的大小不仅由煤有机质的初始性质决定,还与煤的升温速率有关^[54];相对较小地增加升温速率可降低有机质粘度,从而增加焦的各向异性,反

之,升温速率降低,将增加有机质粘度,各向异性程度减弱,形成各向同性焦^[46]。

5)压力。压力对美国 Purgatoire 河谷 Raton 组热变质煤中镶嵌结构的发育有重要影响^[29];印度 Jharia 煤田热变质煤在过载压力作用下,焦各向异性较实验室碳化焦更明显^[1],XIV 煤层热变质煤的强各向异性与高温和高岩石静压力有关^[16];波兰 Upper Silesian 盆地 Sosnica 矿 416 煤层与辉绿岩-粗面岩岩脉接触带的压力导致各向异性指数较实验室 1 200 ℃ 的碳化焦大^[66]。

2.5 热解碳的发育

2.5.1 热解碳的类型

GOODARZI^[67]将热解碳分为:>80 μm 具各向异性的球状、约 12 μm 弱各向异性球、各向同性囊泡化颗状团聚体和各向异性无固定形态 6 μm 厚层状碳。印度 Jharia 煤田煤层挥发分原位化学裂解形成热解碳,热解碳呈薄层状、穹形、蠕虫状和绳状,具强各向异性,以 1~10 μm 厚的层状衬里形式充填孔隙^[1,16,42];澳大利亚 Collinsville 煤系玢岩侵入煤层,产生的挥发性气体在孔裂隙表面沉积形成薄层热解碳^[37],Black Jack 群辉绿岩侵入煤层,惰质组孔隙表面形成热解碳衬里^[31];美国 Illinois 盆地 Springfield 煤层的热解碳表明热变质过程挥发分被煤和沉积物物理捕集,未释放迁移^[18];南极洲 Transantarctic 山高煤级煤和天然焦中热解碳以多种形态存在,如裂隙衬里、囊泡充填、惰质组外壳等^[64];印尼 Suban 煤层热变质带裂隙中球粒热解碳具辐射状结构,为热解碳的最典型特征^[43];安徽淮北煤田袁店矿天然焦发育具较高反射率和各向异性的微球粒热解碳^[68],朔里矿 5 煤层热变质煤发育球状热解碳(图 4b)^[61];湖南新化县寒婆坳矿区花岗岩侵入石墨化煤中热解碳发育^[69]。

2.5.2 热解碳形成的影响因素

球状热解碳表明其形成过程快速升温且较高温度,而层状热解碳表明其形成时间较长,温度较低^[67,70]。美国 Purgatoire 河谷 Raton 组热变质煤中热解碳以边缘状、层状和球粒状形式存在,源于气相冷凝,表明形成温度至少为 500 ℃^[15],Raton 组煤层上部热变质煤存在热解碳球粒,且具初始镶嵌结构,表明近岩床方向的温度梯度增大^[29];Raton 盆地煤与岩脉接触带热解碳呈典型薄层状和各向同性,表明温度较低,而与岩床接触带的热解碳呈各向异性,表明温度较高,无论岩脉和岩床,热解碳均仅限于接触带距侵入体本身宽度一半的范围内^[60];印度 Jharia 煤田热变质煤由于剧烈的岩浆热作用导致热

解碳沉积^[42];加拿大 Telkwa 热变质煤中含球粒状和层状热解碳,与煤挥发分,主要是焦油的热裂解有关,球粒状热解碳主要存在于与岩脉接触带的天然焦中,表明其形成温度高达 1 000 ℃^[52]。

2.6 石墨球粒的形成

印度 Jharia 煤田 XIV 煤层热变质煤的裂隙和孔隙中存在石墨球粒,呈焦油和沥青状,粒径 0~2.0 μm,具有 Brewster 正交结构^[16],当温度高于 500 ℃,挥发分化学裂解冷却形成石墨球晶和热解碳^[1]。湖南寒婆坳矿区花岗岩侵入石炭系煤层,导致其石墨化,形成细粒状微晶石墨^[69]。

2.7 焦化沥青质的形成

南极洲 Transantarctic 山热变质煤除形成各向同性焦、各向异性镶嵌结构、囊泡结构和热解碳等结构外,还发现焦化沥青质^[64]。

3 结 论

岩浆侵入煤层,由于岩浆高温、侵位煤层增大的压力、热液流体等因素,导致煤结构构造和煤显微组分发生显著改变,形成变质结构,具体包括:

1)煤原始沉积构造改变,韧性变形形成各类变形和褶皱;塑性变形形成不同规模流动构造;或由于冷却体积变化和扩张空间受限发育柱状节理。

2)煤接触热变质过程中,镜质组转变成各向同性或各向异性焦,类脂组消失,而惰质组基本不变。

3)岩浆接触热变质作用伴随的挥发分逸散和温度剧变,导致煤层微孔裂隙发育,形成脱挥发孔或囊状结构;煤有机质变质新形成各向同性焦、各向异性焦、热解碳、石墨球粒和焦化沥青质等结构;初始煤级、煤岩组成、温度、升温速率和压力等对各向同性和各向异性焦结构的形成有重要影响。

致 谢:感谢中国矿业大学(北京)王绍清教授在论文选题、结构设计和文章修改方面给予的宝贵意见和建议;感谢中国矿业大学(北京)王西勃教授提供部分显微煤岩照片。

参考文献(References):

- [1] SINGH A K,SINGH M P,SHARMA M,*et al.* Microstructures and microtextures of natural cookes:a case study of heat-affected coking coals from the Jharia coalfield,India[J]. International Journal of Coal Geology,2007,71(2/3):153~175.
- [2] SAGHAFI A,PINETOWN K L,GROBLER P G,*et al.* CO₂ storage potential of South African coals and gas entrapment enhancement due to igneous intrusions [J]. International Journal of Coal Geology,2008,73(1):74~87.

- [3] GOLAB A N, CARR P F. Changes in geochemistry and mineralogy of thermally altered coal, Upper Hunter Valley, Australia [J]. International Journal of Coal Geology, 2004, 57(3/4): 197–210.
- [4] JIANG J Y, CHENG Y P, WANG L, et al. Petrographic and geochemical effects of sill intrusions on coal and their implications for gas outbursts in the Wolonghu Mine, Huabei Coalfield, China [J]. International Journal of Coal Geology, 2011, 88(1): 55–66.
- [5] YAO Y, LIU D. Effects of igneous intrusions on coal petrology, pore-fracture and coalbed methane characteristics in Hongyang, Handan and Huabei coalfields, North China [J]. International Journal of Coal Geology, 2012, 96/97: 72–81.
- [6] YAO Y, LIU D, HUANG W. Influences of igneous intrusions on coal rank, coal quality and adsorption capacity in Hongyang, Handan and Huabei coalfields, North China [J]. International Journal of Coal Geology, 2011, 88(2/3): 135–146.
- [7] 李恒乐, 张玉贵, 秦勇, 等. 淮北矿区祁东井田中生代岩浆侵入作用对煤层瓦斯赋存的影响 [J]. 煤炭学报, 2015, 38(11): 1982–1987.
- LI H, ZHANG Y, QIN Y, et al. Influence of Mesozoic magmatic intrusion on coalbed gas occurrence in Qidong well field, Huabei mining area [J]. Journal of China Coal Society, 2015, 38(11): 1982–1987.
- [8] SVENSEN H, PLANKE S, MALTHE-SORENSSEN A, et al. Release of methane from a volcanic basin as a mechanism for initial Eocene global warming [J]. Nature, 2004, 429: 542–545.
- [9] MCELWAIN JC, WADE-MURPHY J, HESSELBO SP. Changes in carbon dioxide during an oceanic anoxic event linked to intrusion into Gondwana coals [J]. Nature, 2005, 435: 479–482.
- [10] YALLUP C, EDMONDS M, TURCHYN AV. Sulfur degassing due to contact metamorphism during flood basalt eruptions [J]. Geochimica et Cosmochimica Acta, 2013, 120: 263–279.
- [11] GANINO C, ARNDT N T. Climate changes caused by degassing of sediments during the emplacement of large igneous provinces [J]. Geology, 2009, 37(4): 323–326.
- [12] RETALLACK G J, JAHREN A H. Methane release from igneous intrusion of coal during Late Permian extinction events [J]. The Journal of Geology, 2008, 116(1): 1–20.
- [13] QUADERER A, MASTALERZ M, SCHIMMELMANN A, et al. Dike-induced thermal alteration of the Springfield Coal Member (Pennsylvanian) and adjacent clastic rocks, Illinois Basin, USA [J]. International Journal of Coal Geology, 2016, 166: 108–117.
- [14] RAHMAN M W, RIMMER S M. Effects of rapid thermal alteration on coal: geochemical and petrographic signatures in the Springfield (No. 5) Coal, Illinois Basin [J]. International Journal of Coal Geology, 2014, 131: 214–226.
- [15] RIMMER S M, CRELLING J C, YOKSOULIAN L E. An occurrence of coked bitumen, Raton Formation, Purgatoire River Valley, Colorado, USA [J]. International Journal of Coal Geology, 2015, 141/142: 63–73.
- [16] SINGH A K, SHARMA M, SINGH M P. SEM and reflected light petrography: a case study on natural cokes from seam XIV, Jharia coalfield, India [J]. Fuel, 2013, 112: 502–512.
- [17] RIMMER S M, YOKSOULIAN L E, HOWER J C. Anatomy of an intruded coal, I; effect of contact metamorphism on whole-coal geochemistry, Springfield (No. 5) (Pennsylvanian) coal, Illinois Basin [J]. International Journal of Coal Geology, 2009, 79(3): 74–82.
- [18] YOKSOULIAN L E, RIMMER S M, ROWE H D. Anatomy of an intruded coal, II; effect of contact metamorphism on organic $\delta^{13}\text{C}$ and implications for the release of thermogenic methane, Springfield (No. 5) Coal, Illinois Basin [J]. International Journal of Coal Geology, 2016, 158: 129–136.
- [19] 邵震杰, 任文忠, 陈家良. 煤田地质学 [M]. 北京: 煤炭工业出版社, 1993.
- [20] 张庆龙, 金瞰昆. 济宁煤田金乡勘探区岩浆岩的侵入特征以及对煤层的影响 [J]. 河北建筑科技学院学报, 1999, 16(3): 72–78.
- ZHANG Qinglong, JIN Kankun. Invading characteristics of the magma rock and its influence to the coal layers in Jinxiang exploration area of Jining coalfield [J]. Journal of Hebei Institute of Architectural Science and Technology, 1999, 16(3): 72–78.
- [21] 黄维清, 周俊杰, 郑荣华. 济宁煤田金乡矿区岩浆活动及对煤层煤质的影响 [J]. 中国煤田地质, 2007, 19(5): 16–18.
- HUANG Weiqing, ZHOU Junjie, ZHENG Ronghua. Magmatic activity and its impact to coal seam and coal quality in Jinxiang mining area, Jining coalfield [J]. Coal Geology of China, 2007, 19(5): 16–18.
- [22] 刘桂建. 黄河北煤田岩浆侵入体基本特征 [J]. 中国煤田地质, 1994, 6(2): 30–34.
- LIU Guijian. The characteristics of magmatic intrusion bodies in Huanghebei Coalfield [J]. Coal Geology of China, 1994, 6(2): 30–34.
- [23] 李文前. 豫东地区岩浆活动对煤层结构及煤质的影响 [J]. 煤田地质与勘探, 2014, 42(6): 8–13.
- LI Weiqian. Effects of igneous intrusions on texture and quality of coal seam in eastern Henan Province [J]. Coal Geology and Exploration, 2014, 42(6): 8–13.
- [24] CHEN M Y, CHENG Y P, ZHOU H X, et al. Effects of igneous intrusions on coal pore structure, methane desorption and diffusion within coal, and gas occurrence [J]. Environmental and Engineering Geoscience, 2017, 23(3): 191–207.
- [25] SHI Q, QIN B, LIANG H, et al. Effects of igneous intrusions on the structure and spontaneous combustion propensity of coal: a case study of bituminous coal in Daxing Mine, China [J]. Fuel, 2018, 216: 181–189.
- [26] KWIECINSKA B K, HAMBURG G, VLEESKENS J M. Formation temperatures of natural coke in the lower Silesian coal basin, Poland. Evidence from pyrite and clays by SEM-EDX [J]. International Journal of Coal Geology, 1992, 21(4): 217–235.
- [27] MASTALERZ M, DROBNIAK A, SCHIMMELMANN A. Changes in optical properties, chemistry, and micropore and mesopore characteristics of bituminous coal at the contact with dikes in the Illinois Basin [J]. International Journal of Coal Geology, 2009, 77(3/4): 310–319.
- [28] GUO Q, FINK R, LITTKE R, et al. Methane sorption behaviour of coals altered by igneous intrusion, South Sumatra Basin [J]. Inter-

- national Journal of Coal Geology, 2019, 214: 103250.
- [29] CRELLING J C, DUTCHER R R. A petrologic study of a thermally altered coal from the Purgatoire River Valley of Colorado [J]. Geological Society of America Bulletin, 1968, 79 (10): 1375–1386.
- [30] PODWYSOCKI M H, DUTCHER R R. Coal dikes that intrude lamprophyre sills, Purgatoire River Valley, Colorado [J]. Economic Geology, 1971, 66(2): 267–280.
- [31] GURBA L W, WEBER C R. Effects of igneous intrusions on coalbed methane potential, Gunnedah Basin, Australia [J]. International Journal of Coal Geology, 2001, 46(2/4): 113–131.
- [32] RODRIGUES S, ESTERLE J, WARD V, et al. Flow structures and mineralisation in thermally altered coal from the Moatize Basin, Mozambique [J]. International Journal of Coal Geology, 2020, 228: 103551.
- [33] DAI S, REN D. Effects of magmatic intrusion on mineralogy and geochemistry of coals from the Fengfeng – Handan Coalfield, Hebei, China [J]. Energy and Fuels, 2007, 21(3): 1663–1673.
- [34] QUEROL X, ALASTUEY A, ZHUANG X, et al. Petrology, mineralogy and geochemistry of the Permian and Triassic coals in the Leping area, Jiangxi Province, southeast China [J]. International Journal of Coal Geology, 2001, 48(1/2): 23–45.
- [35] XU C, CHENG Y, WANG L, et al. Experiments on the effects of igneous sills on the physical properties of coal and gas occurrence [J]. Journal of Natural Gas Science and Engineering, 2014, 19: 98–104.
- [36] MAHESH S, MURTHY S, SINGH V P, et al. Thermally altered coals from bore core EBM-1, East Bokaro coal field, Damodar Valley, India: a petrographic inference [J]. Journal of Geological Society of India, 2015, 86: 535–546.
- [37] KISCH H J, TAYLOR G H. Metamorphism and alteration near an intrusive-coal contact [J]. Economic Geology, 1966, 61 (2): 343–361.
- [38] PRESSWOOD S M, RIMMER S M, ANDERSON K B, et al. Geochemical and petrographic alteration of rapidly heated coals from the Herrin (No. 6) Coal Seam, Illinois Basin [J]. International Journal of Coal Geology, 2016, 165: 243–256.
- [39] LI K, RIMMER S M, PRESSWOOD S M, et al. Raman spectroscopy of intruded coals from the Illinois Basin: correlation with rank and estimated alteration temperature [J]. International Journal of Coal Geology, 2020, 219: 103369.
- [40] RAHMAN M W, RIMMER S M, ROWE H D. The impact of rapid heating by intrusion on the geochemistry and petrography of coals and organic-rich shales in the Illinois Basin [J]. International Journal of Coal Geology, 2018, 187: 45–53.
- [41] THORPE A N, SENFTLE F E, FINKELMAN R B, et al. Change in the magnetic properties of bituminous coal intruded by an igneous dike, Dutch Creek Mine, Pitkin County, Colorado [J]. International Journal of Coal Geology, 1998, 36(3/4): 243–258.
- [42] SINGH A K, SHARMA M, SINGH M P. Genesis of natural cokes: some Indian examples [J]. International Journal of Coal Geology, 2008, 75(1): 40–48.
- [43] AMIJAYA H, LITTKER R. Properties of thermally metamorphosed coal from Tanjung Enim Area, South Sumatra Basin, Indonesia with special reference to the coalification path of macerals [J]. International Journal of Coal Geology, 2006, 66(4): 271–295.
- [44] GROCKE D R, RIMMER S M, YOKSOULIAN L E, et al. No evidence for thermogenic methane release in coal from the Karoo–Ferrar large igneous province [J]. Earth and Planetary Science Letters, 2009, 277(1/2): 204–212.
- [45] VARGA E, HORVATH Z. Coal petrographical characterization of the Mecsek bituminous coal basin, with special reference to the contact metamorphism of coal seams [J]. International Journal of Coal Geology, 1986, 6(4): 381–391.
- [46] WARD C R, WAR BROOKE P R, ROBERTS F I. Geochemical and mineralogical changes in a coal seam due to contact metamorphism, Sydney Basin, New South Wales, Australia [J]. International Journal of Coal Geology, 1989, 11(2): 105–125.
- [47] QUEROL X, ALASTUEY A, LOPEZ-SOLER A, et al. Geological controls on the mineral matter and trace elements of coals from the Fuxin basin, Liaoning Province, northeast China [J]. International Journal of Coal Geology, 1997, 34(1–2): 89–109.
- [48] GHOSH T K. A study of temperature conditions at igneous contacts with certain Permian coals of India [J]. Economic Geology, 1967, 62(1): 109–117.
- [49] CHAKRABARTI A K. On the effects of igneous intrusion on a few coal seams of the Jharia coal field, Bihar, India [J]. Economic Geology, 1969, 64(3): 319–324.
- [50] MERRITT R D. Thermal alteration and rank variation of coals in the Matanuska field, south-central Alaska [J]. International Journal of Coal Geology, 1990, 14(4): 255–276.
- [51] SNYMAN C P, BARCLAY J. The coalification of South African coal [J]. International Journal of Coal Geology, 1989, 13(1/4): 375–390.
- [52] GOODARZI F, CAMERON A R. Organic petrology and elemental distribution in thermally altered coals from Telkwa, British Columbia [J]. Energy Sources, 1990, 12(3): 315–343.
- [53] 马宏涛, 宋晓夏, 李凯杰, 等. 大同煤田接触变质煤的煤岩煤质变化规律 [J]. 煤田地质与勘探, 2020, 48(2): 99–105.
- MA H, SONG X, LI K, et al. Changes of petrographic characteristics and quality of contact-metamorphosed coals in the Datong coalfield [J]. Coal Geology and Exploration, 2020, 48 (2): 99–105.
- [54] JONES J M, CREANEY S. Optical character of thermally metamorphosed coals of northern England [J]. Journal of Microscopy, 1977, 109(1): 105–118.
- [55] GOLAB A N, HUTTON A C, FRENCH D. Petrography, carbonate mineralogy and geochemistry of thermally altered coal in Permian coal measures, Hunter Valley, Australia [J]. International Journal of Coal Geology, 2007, 70(1/3): 150–165.
- [56] RAHMAN M W, RIMMER S M, ROWE H D, et al. Carbon isotope analysis of whole-coal and vitrinite from intruded coals from the Illinois Basin: No isotopic evidence for thermogenic methane generation [J]. Chemical Geology, 2017, 453: 1–11.
- [57] 宋晓夏, 马宏涛, 李凯杰, 等. 大同煤田石炭-二叠系接触变质煤的煤岩学特征研究 [J]. 煤炭科学技术, 2020, 48(12): 182–

- 191.
- SONG X, MA H, LI K, et al. Study on coal petrology characteristics of contact metamorphosed coal from Carboniferous-Permian in Datong Coalfield [J]. Coal Science and Technology, 2020, 48(12): 182-191.
- [58] STEWART A K, MASSEY M, PADGETT P L, et al. Influence of a basic intrusion on the vitrinite reflectance and chemistry of the Springfield (No. 5) coal, Harrisburg, Illinois [J]. International Journal of Coal Geology, 2005, 63(1/2): 58-67.
- [59] SCHIMMELMANN A, MASTALERZ M, GAO L, et al. Dike intrusions into bituminous coal, Illinois Basin; H, C, N, O isotopic responses to rapid and brief heating [J]. Geochimica et Cosmochimica Acta, 2009, 73(20): 6264-6281.
- [60] COOPER J R, CRELLING J C, RIMMER S M, et al. Coal metamorphism by igneous intrusion in the Raton Basin, CO and NM: Implication for generation of volatiles [J]. International Journal of Coal Geology, 2007, 71(1): 15-27.
- [61] WANG X, JIANG Y, ZHOU G, et al. Behavior of minerals and trace elements during natural coking: a case study of an intruded bituminous coal in the Shuoli Mine, Anhui Province, China [J]. Energy and Fuels, 2015, 29(7): 4100-4113.
- [62] 汪米娜, 安燕飞, 何凯, 等. 皖北石台矿岩浆蚀变煤中有毒元素分布、赋存及富集机理 [J]. 矿物岩石地球化学通报, 2019, 38(6): 1118-1128.
- WANG M, AN Y, HE K, et al. Distribution, occurrence and enrichment mechanism of toxic elements in altered coals by magmatic intrusion in the Shitai Coal Mine, northern Anhui [J]. Bulletin of Mineralogy, Petrology and Geochemistry, 2019, 38(6): 1118-1128.
- [63] 赵继尧. 安徽省淮北闸河矿区煤的岩浆热变质作用的几个问题 [J]. 煤炭学报, 1986, (4): 19-27.
- ZHAO J. Some aspects of magmatic thermal metamorphism of coal in Zhahe mine area, Huaipei, Anhui Province [J]. Journal of China Coal Society, 1986, (4): 19-27.
- [64] SANDERS M M, RIMMER S M. Revisiting the thermally metamorphosed coals of the Transantarctic Mountains, Antarctica [J]. International Journal of Coal Geology, 2020, 228: 103550.
- [65] GOODARZI F, MURCHISON D G. Optical properties of carbonized vitrinites [J]. Fuel, 1972, 51(4): 322-328.
- [66] MATUSZEWSKA A, PUSZ S, DUBER S. Evaluation of the structure of bituminous coal from Sonica mine in the Upper Silesian Coal Basin (Poland) using reflectance indicating surface (RIS) parameters [J]. International Journal of Coal Geology, 2015, 152: 177-188.
- [67] GOODARZI F. Characteristics of pyrolytic carbon in Canadian coals [J]. Fuel, 1985, 64(12): 1672-1676.
- [68] AN Y, LIU L, WANG M, et al. Source and enrichment of toxic elements in coal seams around mafic intrusions: constraints from pyrites in the Yuandian Coal Mine in Anhui, eastern China [J]. Minerals, 2018, 8(4): 164.
- [69] LI K, RIMMER S M, LIU Q. Geochemical and petrographic analysis of graphitized coals from Central Hunan, China [J]. International Journal of Coal Geology, 2018, 195: 267-279.
- [70] GOODARZI F, GENTZIS T, GRASBY S E, et al. Influence of igneous intrusions on thermal maturity and optical texture: Comparison between a bituminous marl and a coal seam of the same maturity [J]. International Journal of Coal Geology, 2018, 198: 183-197.